Psychosine remodels model lipid membranes at neutral pH

Yenisleidy de las Mercedes Zulueta Díaz[a,b], Sofia Caby[a], Ernesto R. Bongarzone[c,d], María Laura Fanani[a,b,*]

[a] Departamento de Química Biológica Ranwel Caputto, Facultad de Ciencias Químicas, Universidad Nacional de Córdoba, Córdoba, Argentina
[b] Centro de Investigaciones en Química Biológica de Córdoba (CIQUIBIC), CONICET, Ciudad Universitaria, Haya de la Torre y Medina Allende, Córdoba X5000HUA, Argentina
[c] Department of Anatomy and Cell Biology, College of Medicine, University of Illinois at Chicago, Chicago, IL 60612, United States of America
[d] Departamento de Química Biológica, IQUIFIB, Universidad Nacional de Buenos Aires, Buenos Aires, Argentina

ABSTRACT

β-Galactosylsphingosine or psychosine (PSY) is a single chain sphingolipid with a cationic group, which is degraded in the lysosome lumen by β-galactosylceramidase during sphingolipid biosynthesis. A deficiency of this enzyme activity results in Krabbe's disease and PSY accumulation. This favors its escape to extralysosomal spaces, with its pH changing from acidic to neutral. We studied the interaction of PSY with model lipid membranes in neutral conditions, using phospholipid vesicles and monolayers as classical model systems, as well as a complex lipid mixture that mimics the lipid composition of myelin. At pH 7.4, when PSY is mainly neutral, it showed high surface activity, self-organizing into large structures, probably lamellar in nature, with a CMC of 38 ± 3 μM. When integrated into phospholipid membranes, PSY showed preferential partition into disordered phases, shifting phase equilibrium. The presence of PSY reduces the compactness of the membrane, making it more easily compressible. It also induces lipid domain disruption in vesicles composed of the main myelin lipids. The surface electrostatics of lipid membranes was altered by PSY in a complex manner. A shift to positive zeta potential values evidenced its presence in the vesicles. Furthermore, the increase of surface potential and surface water structuring observed may be a consequence of its location at the interface of the positively charged layer. As Krabbe's disease is a demyelinating process, PSY alteration of the membrane phase state, lateral lipid distribution and surface electrostatics appears important to the understanding of myelin destabilization at the supramolecular level.

1. Introduction

Psychosine or β-galactosylsphingosine (PSY) (Scheme 1) is an intermediate in the biosynthesis of sphingolipids, occurring in the lysosome lumen. It is degraded by the enzyme β-galactosylceramidase. A deficiency of this enzyme activity results in the progressive accumulation of PSY, 10- to 100-fold above its normal concentration [1], being responsible for so-called globoid cell leukodystrophy or Krabbe's disease. This is an inherited autosomal disorder that leads to demyelination, infiltration of macrophages into the brain parenchyma and early death [2]. PSY is a highly cytotoxic glycolipid in the 20–50 μM range [3]. Its mechanism of toxicity appears to occur through pleiotropic factors, including dysfunctions in several metabolic pathways [4]. There is evidence that this amphiphilic molecule exerts its pathological effect by partitioning into membranes and affecting their function [1,3,5,6]. It is also known that PSY is hemolytic [4] and induces

Scheme 1. Chemical structure of β-galactosylsphingosine or psychosine (PSY). The ionizable amine group with a pKa of 7.18 is highlighted.

permeabilization of liposomes [3].

Typically, biomembranes contain 10–16 mol% of negatively charged lipids [7], meaning that cell membranes are anionic. Natural cationic lipids are very rare and are present in very low quantities in physiological conditions. As far as we know, they are circumscribed to a few single chain sphingolipids, such as sphingosine (SPH), sphinganine and their glycosylated derivatives, glycosylsphingosine and PSY [4,8]. SPH has an apparent pKa of 9.1, and thus is cationic in the pH range that concerns physiological environments. On the other hand, PSY show a pKa of 7.18 [9], indicating that, in its natural environment - the acidic lysosomal lumen, PSY is mainly charged. At pH 4.5, PSY behaves as a mild soluble amphiphile, organized as micelles of ~14 nm in diameter and a critical micellar concentration (CMC) of 1.26 mM [9]. However, in Krabbe's disease, PSY is present at high concentrations and escapes the lysosome lumen to accumulate in extralysosomal spaces, such as the cytoplasm or extracellular milieu, at pH close to neutrality (~7.4). At this pH, PSY is only partially charged, forming stable Langmuir films [10] and large structures in bulk, whilst its CMC drops to the micromolar range [9]. Its properties then differ from those of the fully charged lipid and a more lipid-like character may prevail.

This work explores the interaction of PSY with model lipid membranes in neutral pH conditions. We used phospholipid membranes in different phase states as classical model systems. Additionally, we explored PSY interaction with a complex lipid mixture of phospholipids, sphingolipids and cholesterol that mimics the lipid composition of myelin [11–13]. As Krabbe's disease is a demyelinating process, our results are relevant to the supramolecular interpretation of the mechanism of biomembrane perturbation by PSY.

2. Materials and methods

2.1. Chemicals and reagents

1-Palmitoyl-2-oleoyl-sn-glycero-3-phosphocholine (POPC), 1,2-dipalmitoyl-sn-glycero-3-phosphocholine (DPPC), 1,2-dimiristoyl-sn-glycero-3-phosphocholine (DMPC). 1,2-Dioleoyl-sn-glycero-3-phosphoethanolamine (DOPE), 1,2-dioleoyl-sn-glycero-3-phospho-L-serine (sodium salt) (DOPS), brain sphingomyelin (bSM), cholesterol (CHO) and 1-β-galactosyl-sphing-4-enine (psychosine or PSY) and 1,2-dioleoyl-sn-glycero-3-phosphoethanolamine-N-(lissamine rhodamine B sulfonyl) (PE-Rho) were purchased from Avanti Polar Lipids, Inc. (Alabama, U.S.A.). Sulfatide (SULF), galactosyl ceramide (Gal-Cer) and total gangliosides (GANG) were purified from bovine brain as reported in Ref. [10] and were all generously provided by Dr. Bruno Maggio. 1,6-Diphenyl-1,35,-hexatriene (DPH) and 6-dodecanoyl-2-dimethyl-aminopnaphthalene (laurdan) were obtained from Invitrogen (Eugene, Oregon, USA). Chloroform, Methanol, NaCl and Tris-Base were supplied by Merck (Darmstadt, Germany). Deionized water with a resistivity of 18 MΩ cm was obtained from a Milli-Q Gradient System (Millipore, Bedford, MA). The lipid mixture mimicking myelin (MM) was chosen to fit bibliographic data [11,13] as follows: CHO, 38 mol%; POPC, 7 mol%; DOPE, 19 mol%; DOPS, 6 mol%; bSM, 10 mol%; SULF, 5 mol%; Gal-Cer 15 and GANG 1 mol%.

2.2. Methods

2.2.1. Adsorption experiments

The adsorption of PSY into the air-water interface was performed by injection of increasing volumes of a stock solution PSY (30 mM) in ethanol into the aqueous subphase under continuous stirring. The subphase was Tris-HCl 10 mM NaCl 135 mM, pH 7.4. A miniature circular trough of 1 mL and 3.14 cm^2 was used for surface tension/pressure measurements coupled to a Langmuir film balance (Kibron MicroTrough, Helsinki, Finland). The change in surface pressure was registered as a function of time. The surface activity curves were fitted via non-linear least-squares regression analysis as follows:

$$\Gamma = \frac{C}{RT}\frac{d\pi}{dC}, \tag{1}$$

where Γ is the amphiphile surface excess concentration, R is the gas constant, T is the temperature, C is the subphase amphiphile concentration and π is the surface pressure defined as the difference between the surface tension of the bare air/buffer interface and the surface tension reached after equilibration with the amphiphile added to the subphase

$$(\pi = \gamma_0 - \gamma), \tag{2}$$

From the maximum Γ value, the area occupied by a single amphiphile molecule at maximal surface concentration can be calculated as:

$$A = \frac{1}{N\Gamma_{max}}, \tag{3}$$

where N is Avogadro's constant. All experiments were performed at 22 ± 1 °C.

2.2.2. Surface titration experiments

The PSY uptake capacity by lipid monolayers at 30 mN/m was tested by means of surface titration experiments [14]. We spread a known amount of lipids onto the air/saline solution surface (at constant area) up to 30 mN/m and then stepwise co-spread a chloroform solution of PSY, registering the resultant π increase after solvent evaporation. At a certain amount of PSY added, a saturating π value was reached, which did not increase with further addition of drug. We determined the PSY mole fraction at which the π reached 50% of the saturating value (X_{50}).

2.2.3. Surface pressure-area isotherms

Monomolecular lipid films were obtained by spreading adequate aliquots of chloroform solutions of lipids onto the aqueous surface of a Teflon™ trough incorporated in a KSV NIMA minitrough equipment (Biolin Scientific AB, Västra Frölunda Sweden). The surface pressure was determined with a Pt plate using the Wilhelmy method. After solvent evaporation and relaxation at π ≤ 0.5 mN/m (~5 min), the film was compressed isometrically at a rate of 6 ± 1 Å^2·molec^{-1}·min^{-1} until reaching the collapse pressure by reducing the area between two Delrin™ barriers. Their lateral movement over the trough surface was controlled and registered by an electronic unit. The mean molecular area (MMA) was taken as the total monolayer area divided by the total number of molecules placed at the interface. The absence of surface-active impurities in the subphase solutions or in the spreading solvents was checked routinely. Surface elasticity upon compression was assessed by means of the compressibility modulus (Cs^{-1}), which was calculated from the isotherm data as [15]:

$$C_s^{-1} = -MMA\left(\frac{\delta\pi}{\delta MMA}\right)_T \tag{4}$$

The surface potential of the film was simultaneously measured with a surface ionizing electrode formed by a ^{241}Am plate positioned ~5 mm above the monolayer surface, and a reference Ag/AgCl$_2$ (3 M) electrode connected to the aqueous subphase.

2.2.4. Brewster angle microscopy

The monolayers were observed while compressed, using a Langmuir KSV NIMA minitrough mounted on the stage of a Nanofilm EP3 Imaging Ellipsometer (Accurion, Goettingen,Germany), which was used in the Brewster angle microscopy (BAM) mode. Zero reflection was set with a polarized laser (λ = 532 nm) incident on the bare aqueous surface at the experimentally calibrated Brewster angle (≈ 53.1°). After monolayer formation and compression, the reflected light was collected with a 20× objective. The gray level of each pixel of the BAM images corresponds to reflectivity values after calibration factors tested for each experiment. The reflectivity is in turn related to the film thickness and the refraction index of the film [16]. The average gray level of the images was calculated using the free software, ImageJ 1.43u (NIH, USA).

2.2.5. Liposome preparation and fluorescence analysis

Multilamellar vesicles (MLVs) were prepared by generating a uniform lipid film on the wall of a glass test tube, by solvent evaporation under a N_2 stream, from a chloroform lipid solution. Traces of solvent were removed during 2 h treatment in a high vacuum chamber. The lipids were hydrated with a buffer solution containing Tris-HCl 5 mM (pH 7.4), applying vigorous mixing and then subjected to five freezing-thawing cycles (−195 °C and 60 °C, respectively). Large unilamellar vesicles (LUVs) with an average diameter of 100 nm were prepared by extrusion (21 times) of MLVs through polycarbonate filters of 100 nm pore size at room temperature. For fluorescence measurements, appropriate aliquots of the fluorescent probes Laurdan or DPH dissolved in dimethyl sulfoxide and choloroform:methanol mixtures, respectively, were added to the chloroform lipid suspension, reaching 1 mol%.

Laurdan generalized polarization (GP) was calculated according to the expression:

$$GP = \frac{(I_{434} - I_{490})}{(I_{434} + I_{490})},\qquad(5)$$

where I_{434} and I_{490} are the typical dye fluorescence emission intensity peaks when Laurdan is mixed with phospholipids, adopting a gel phase or a liquid-crystalline phase, respectively. The excitation wavelength was 360 nm. From Eq. (5), it can be deduced that high Laurdan GP values correspond to laterally ordered phases (gel-like), whereas low Laurdan GP values correspond to fluid phases.

Fluorescence anisotropy was measured in the T format with Schott KV418 filters in the emission channels and corrected for optical distortions and background signals. The excitation and emission wavelengths used were 365 and 425 nm, respectively. The anisotropy value, r, was obtained according to the following equation [17]:

$$r = \frac{\left(\frac{I_v}{I_h}\right)_v - \left(\frac{I_v}{I_h}\right)_h}{\left(\frac{I_v}{I_h}\right)_v + 2\left(\frac{I_v}{I_h}\right)_h},\qquad(6)$$

associating the ratios of the intensities of emitted vertically (v) or horizontally (h) polarized light to the exciting vertically or horizontally polarized light, respectively. The fluorescence measurements were acquired with a Cary Eclipse spectrofluorometer (Agilent Technologies) equipped with a thermally controlled multi-cuvette holder (21 °C), setting the wavelength slit at 5 nm and using a 2 mm path cuvette.

2.2.6. Particle analysis

The size-distribution of particles was studied by dynamic light scattering using a 530 nm laser beam, and analyzed at 90 °C through the adjustment of a correlation function. The hydrodynamic diameter of the particles was determined by the Stokes-Einstein equation. The equipment used was a Nicomp™ 380 Submicron Particle Sizer (Santa Barbara, California, USA). Zeta potential measurements were performed using the Zetasizer SZ-100-Z equipment (Horiba, Ltd., Japan), provided with a semiconductor laser excitation solid state (532 nm, 10 mW) and using

the laser-Doppler velocimetry technique. The lipid particles were suspended in 5 mM Tris-HCl, pH 7.4 at a final lipid concentration of 0.4 mM.

2.2.7. Confocal microscopy visualization of giant unilamellar vesicles (GUVs)

GUVs were prepared by the electroformation method. Briefly, 7 μL of a lipid or lipid/PSY solution (0.5 mg/mL in Chloroform:Methanol 2:1 v/v), doped with 0.5 mol% of the fluorescent probe PE-Rho, were spread onto two stainless steel plates as described in [18]. The plates were subjected to vacuum (1 h) to remove any remaining traces of organic solvent. The lipids were hydrated with a 300 mOsm sucrose solution previously filtered and heated to 60 °C. The electrodes were connected to a homemade function generator applying potential for 1 h at 37 °C for DMPC or 2 h at 45 °C for MM vesicles, respectively. Initially, a sine wave potential of 10 Hz was applied, with amplitude from 0 to 2.6 V peak to peak potential increasing linearly in 60 s (Bartlett modulation), which was afterwards maintained at 2.6 V peak to peak potential [18].

A small aliquot of the GUV suspension (20 μL) was transferred to an 8-well observation chamber (Lab-Tek, Thermo Fisher Scientific, Inc. NYSE:TMO) and diluted 10-fold with 300 mOsm Tris-HCl buffer. The sucrose and Tris-HCl buffer solutions were checked for isosmolarity with an Automatic Micro-Osmometer OM-806, (VOGEL GmbH & Co. KG, Giessen, Germany). Before GUV addition to the well, the glass of the observation chamber was treated with a 10 mg/mL β casein solution, which prevented GUV rupture onto the slide. The excess of β casein was eliminated by several washes with Tris-HCl buffer. The giant liposomes where observed with a fluorescence confocal microscope (Olympus FV 300, Tokyo, Japan). Confocal Images of GUVs were processed and quantified with the FIJI ImageJ software (NIH, USA).

3. Results and discussion

3.1. Characterization of PSY suspension at neutral pH

An increasing concentration of PSY induces adsorption of the molecules to the air/water interface, lowering the surface tension (Fig. 1A). This process follows the Gibbs adsorption equation (Eq. (1)) until the system reaches the CMC (see arrow in Fig. 1A). From the fitting of the data with Eq. (1) and applying Eq. (3), the mean molecular area (MMA) occupied by PSY at the interface could be estimated. This analysis gives a value of 43 ± Å^2/molecule, an area larger by 40% than the MMA obtained by compression isotherms of Langmuir films (23 ± 2 Å^2/molecule) [10]. This suggests that the organization of PSY at the interface after spontaneous adsorption (forming Gibbs monolayers) results in a less compacted film than that obtained by compression of Langmuir films.

Our results shown in Fig. 1A give a value of 38 ± 3 μM, for the CMC, which matches the concentration range reported by Orfi et al. of 20–300 μM [9]. These authors used electron microscopy to find a mixture of small structures, 15–23 nm in size, regarded as micelles with larger elongated structures > 100 nm. We studied PSY suspension at neutral pH by Dynamic Light Scattering and we also found the presence of micelles < 20 nm (note that the equipment's lower detection limit is 10 nm) coexisting with large structures in the micrometer range (0.6–3.3 μm) (Fig. 1B).

It is also worth noting that the volume (and amount of molecules) of PSY organized in micelles was almost negligible compared with the amount composing the micro-size structures. Compared to the fully charged situation at pH 4.5, a lower intermolecular electrostatic repulsion must occur when PSY is only partially charged, which may favor its organization into a more compact structure, probably of a lamellar nature, that results in large aggregates. This result resembles early observations by Hargreaves and Deamer of liposome formation (lamellar phase) in fatty acid diluted solutions when they are mainly
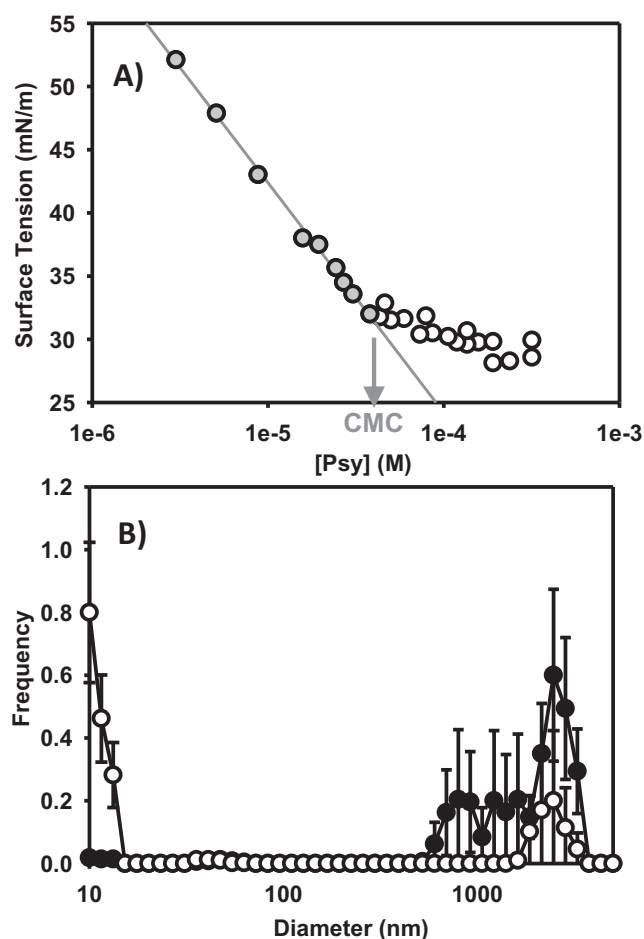
Fig. 1. Characterization of PSY suspension in buffer solution at pH 7.4. A) Surface tension decrease after PSY interfacial adsorption. Gray symbols and gray line highlight the portion of the curve that follows Eq. (1). The arrow indicates the CMC value of 38 ± 2 μM. The regression line was adjusted to the data corresponding to two independent experiments. B) Size distribution of particles in a 50 μM PSY suspension analyzed by dynamic light scattering. The analysis was performed considering the particle volume (black symbols) or number (open symbols). The frequency axes indicate the relative distribution, ranging from 0 to 1 for all cases. Error bars correspond to the Standard Error of the Mean (SEM) of five independent experiments. T: 22 ± 1 °C.

present in the protonated form [19]. These authors stated that short- and long-chain saturated fatty acids as well as oleic acid can form liposomes that behave similarly in many respects to those formed from biological phospholipids. On the other hand, other single-chain sphingolipids have been reported to form lamellar phases. In the fully protonated form, at pH 6.0, SPH exhibits a thermotropic transition centered at 30 °C, whilst it is shifted to 39 °C at pH above its pKa (9.1) [8]. Additionally, *N*-acetyl-galactosylsphingosine has been found to form only lamellar phases before melting to the fluid isotropic phase at very high temperatures (> 54 °C) [20]. This picture is in accordance with the fact that PSY accumulates in the brain of Krabbe's disease patients, an unlikely situation for an amphiphile that prefers micellar organization.

3.2. PSY interaction with lipid monolayers

We used Langmuir monolayers as model lipid membranes. This allows a continuous monitoring of parameters such as surface pressure (π), which is the extent of the lowering of surface tension by the presence of the lipid film (see Eq. (2)), molecular packing and elasticity of the film. The latter parameter gives information about its phase state
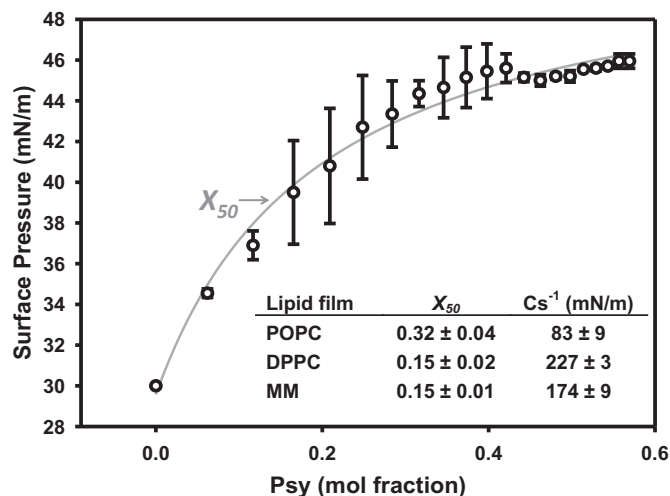

Fig. 2. Surface titration of lipid monolayers by PSY. The surface pressure reached after stepwise addition of PSY into the myelin-like mixture (MM) monolayer initially at 30 mN/m and at constant area, as a function of the resultant mole fraction of PSY. The arrow illustrates the mole fraction necessary to reach 50% of the saturation surface pressure (X_{50}). The regression line represents the adjustment of a hyperbolic function to the data. The values are the average of two independent experiments and the error bars represent the SEM. The table shows the values of X_{50} and compressibility modulus (Cs^{-1}) for lipid films of the indicated composition at 30 mN/m (for the last parameter no PSY added).

[21]. The addition of an amphiphile to a pre-established lipid film at constant area results in an increase of π until reaching saturation [15]. This behavior was also found for PSY against three different lipid films (Fig. 2). Two zwitterionic phospholipids were chosen as model membranes, palmitoyl-oleoyl-phosphatidylcholine (POPC) and dipalmitoyl-phosphatidylcholine (DPPC), which show expanded or compact phases, respectively, at room temperature both in monolayer or bilayer organization [7,22]. When organized in Langmuir films, POPC is at a liquid-expanded (LE) phase and shows values of compressibility modulus (Cs^{-1}) < 100 mN/m, as shown in the inset of Fig. 2. On the other hand, DPPC monolayers at 30 mN/m show Cs^{-1} values > 100 mN/m, which evidences a liquid-condensed (LC) phase state [23]. Additionally, a complex mixture was used that mimics the lipid composition of myelin (MM) (see Chemicals and reagents section). It contains glycerophospholipids, sphingolipids and a considerable content of cholesterol (CHO) [11,12]. The latter provides a relatively high Cs^{-1} value to this mixture (inset in Fig. 2), a finding typically observed in membranes with a high content of CHO, which present liquid-ordered (LO) phases [24].

Surface titration of lipid monolayers by PSY resulted in a saturation effect, as shown in Fig. 2, which can be described by a hyperbolic function. The amount of PSY necessary to reach 50% of the saturation π is reported as the mole fraction X_{50} (see inset in Fig. 2). POPC monolayers allowed a larger uptake of PSY than DPPC and MM films. This agrees with previous observations that the phase state of the hosting film modulates the incorporation of other amphiphiles such as amphipathic drugs [14,25]. In this context, the inclusion of a PSY molecule in the film induces lateral compression of the other membrane components, which in turn counteract this pressure according to the film elasticity. Thus, a membrane in the LE phase, which shows a low Cs^{-1}, can accommodate a larger amount of PSY molecules than the more compact ones.

To further test this hypothesis, we extended this study to the effect of PSY on heterogeneous membranes. The preferential lateral mixing of PSY was evaluated on DPPC membranes, which show LE/LC phase coexistence in the 5–17 mN/m pressure range [25,26]. Another advantage of working with Langmuir films as model lipid membranes is
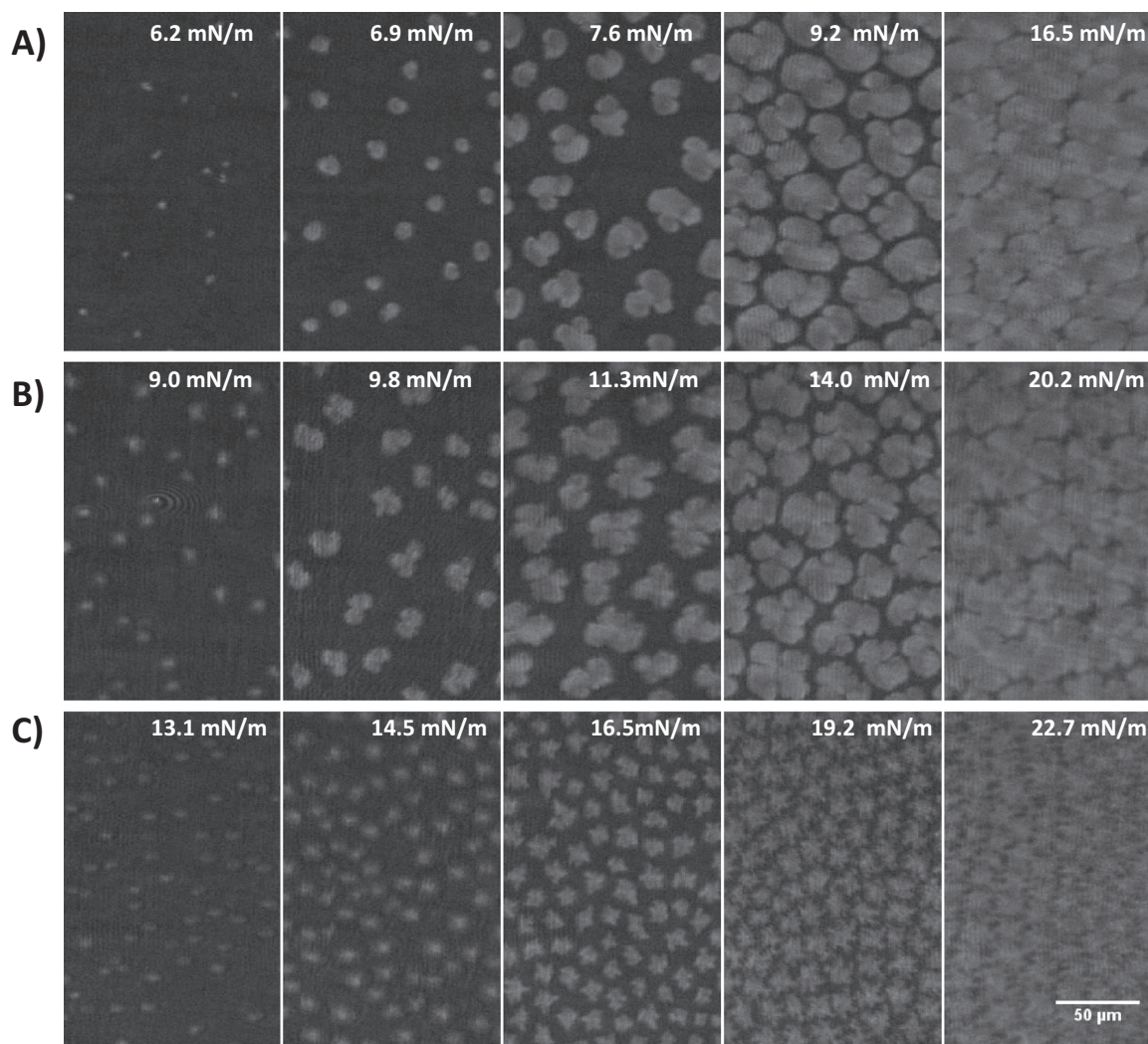
Fig. 3. Brewster angle microscopy and compression isotherms of mixed Langmuir monolayers of DPPC and PSY. Micrographs of pure DPPC (A) or DPPC containing 10 (B) or 25 mol% (C) of PSY are shown at the surface pressures indicated. For better visualization, the background was subtracted and the gray level of the images was modified selecting the range 0–100 from the original 0–255 scale. T: 22 ± 1 °C. The images correspond to a single experiment, which is representative of two independent trials.

that their microstructure can be assessed continuously during the film compression, in a probe-free experiment by Brewster angle microscopy (BAM). Since the gray level of BAM images increases with both monolayer thickness and the refraction index of the film [16], the LE phase appears as darker regions in the image in comparison with LC domains, which show a more compact and/or thicker nature (Fig. 3).

DPPC formed LE films at $\pi < 5$ mN/m, and above this π an LC phase nucleated and grew upon compression, forming curved-branched domains. This particular shape responds to the DPPC chiral structure, which defines a preferential growing vector in the two-dimensional crystal [26]. BAM imaging revealed optical anisotropy due to a tilted arrangement of the ordered acyl chains of DPPC in its crystalline structure [27]. This effect results in the most distal part of the branches appearing brighter than the more proximal part (Fig. 3A). A near-uniform phase of LC character was observed at $\pi > 17$ mN/m, which conserved the anisotropic organization. This phase transition can also be observed by inspection of the compression isotherm of the film (see Fig. S1A, in Supplementary material - I), where a kink occurs at ~5 mN/m. This marks the beginning of the phase transition, and a near-plateau is established during the phase transition progress (mean molecular area [MMA] range of 50–70 Å^2/molecule). As a comparison, PSY Langmuir films did not show phase transition and showed

characteristics of a LE phase (Fig. S1A and B) in all the compression process, as previously reported [10].

The addition of 10 or 25 mol% of PSY to the lipid film altered the phase equilibrium of the system as well as its surface texture. The progressive increase in PSY content shifted the beginning of the phase transition to higher π (from 6.4 ± 0.1 mN/m for pure DPPC to 12.5 ± 0.1 mN/m for 25 mol% PSY). This is evidenced by BAM images in Fig. 3 and by independent measurement of the compression isotherm (Fig. S1A, B). To highlight this effect, the average gray value of all the images acquired in each experiment was analyzed and is shown in Fig. S1C, where the burst indicates the appearance of LC domains. This effect indicates a preferential partition of PSY for the LE phase, thermodynamically stabilizing this phase and altering the phase equilibrium.

On the other hand, when a high proportion of PSY was present, it also affected the properties of the LC phase. This is concluded from the change in the structure of the LC domains from curved branched to star-like (compare Fig. 3A and C). This effect may be a consequence of higher intra-domain repulsion [28] due to the presence of a partially charged molecule: PSY. This change in LC phase property was also evidenced by the lowering of the Cs^{-1} from 227 ± 3 (pure DPPC) to 94 ± 4 mN/m (25 mol% PSY) at 30 mN/m (see Fig. S1B at low MMA).

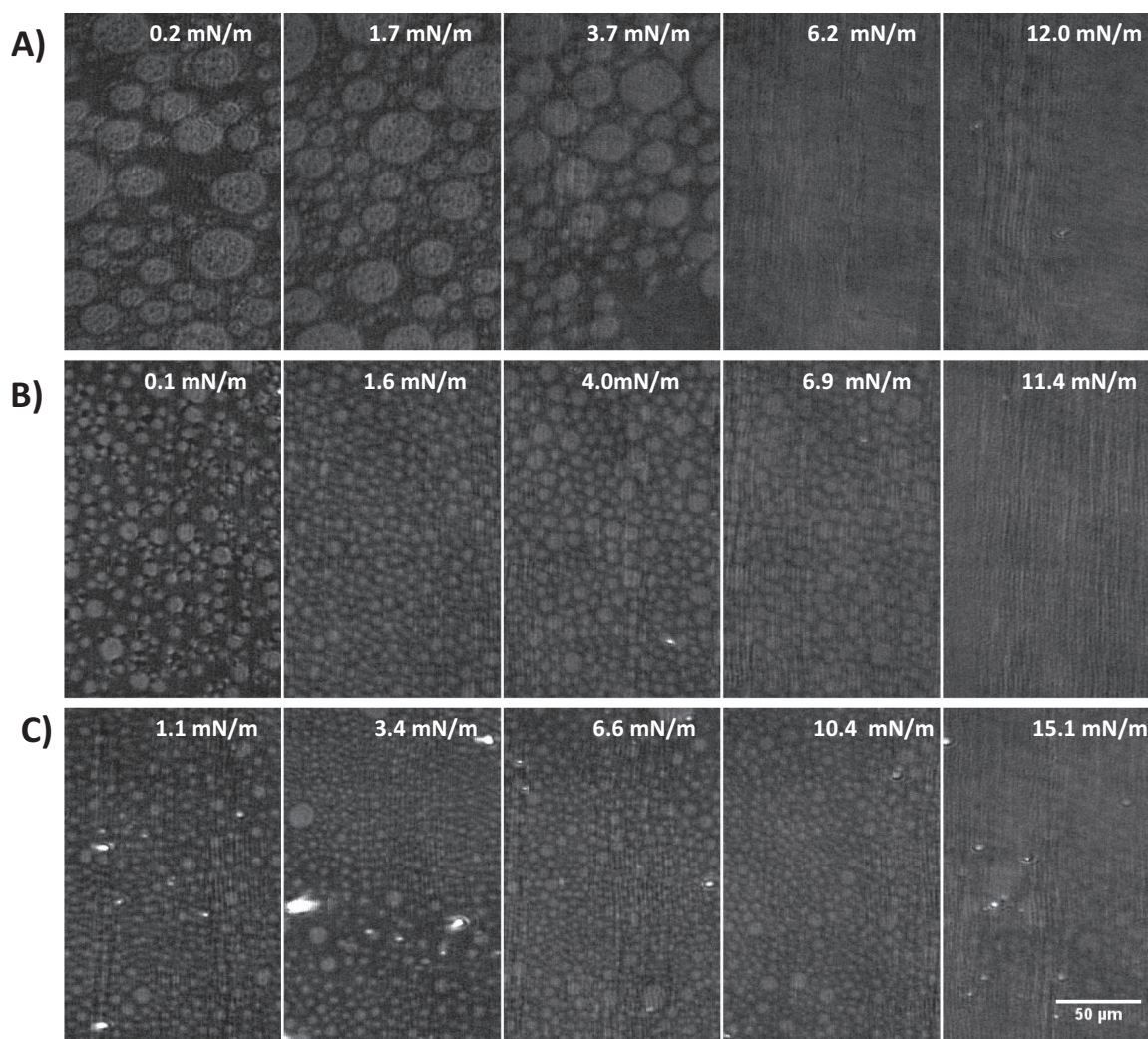The effect of PSY was also analyzed in a second heterogeneous lipid

Fig. 4. Brewster angle microscopy of Langmuir monolayers of the myelin-like mixture (MM) in the absence or presence of PSY. Micrographs of MM (A) or MM containing 10 (B) or 25 mol% (C) of PSY are shown at the surface pressures indicated. For better visualization, the background was subtracted and the gray level of the images was modified selecting the range 0–60 from the original 0–255 scale. T: 22 $\pm$ 1 °C. The images correspond to a single experiment, which is representative of two independent trials.

system. The myelin-mimicking mixture (MM) showed coexistence of LE and a brighter phase with rounded domains at low π (Fig. 4A). This is the typical pattern for liquid-liquid coexistence and the brighter phase corresponds to the CHO-enriched LO phase [24]. Upon compression, the phases merged at the miscibility transition π, probably due to the reduction of the compositional miscibility gap [24], resulting in a homogeneous film.

As expected for a film containing a high proportion of CHO, its compression isotherm showed a sharp vertical slope above its miscibility transition π, revealing a compact surface organization (Fig. S2, in Supplementary material - I)). This behavior matches that observed for Langmuir films formed by extracted natural myelin membranes [11,29].

The presence of PSY induced a shift of the merging π to higher values (from 5.3 $\pm$ 0.4 for MM to 16.2 $\pm$ 0.4 mN/m for MM + 25 mol % PSY, see Fig. 4). This again evidenced a preferential partition of PSY to one of the phases, increasing the compositional gap between both phases and favoring phase separation. According to its LE character, PSY also induced a lowering in Cs^{-1} values for monolayers of MM at high π (from 174 $\pm$ 9 for MM to 106 $\pm$ 2 mN/m for MM + 25 mol% of PSY at a π = 30 mN/m, see Fig. S2B).

On the other hand, when PSY was mixed with POPC (in an LE

phase), the resulting film showed a homogeneous character (not shown). This, together with the larger X_{50} found for LE films than for compact ones in surface titration experiments, suggests that, when PSY is placed in a heterogeneous film (such as MM), it may be preferentially present in the LE rather than in the LO phase. Supporting this hypothesis is the finding reported by Maggio et al. [12] that all the charged components analyzed in films of myelin extracts are present in the LE phase, while only neutral components are found in the LO phase. This is expected since in-plane electrostatic repulsion will prevent the occurrence of a highly compact lateral organization such as that present in the LO phase.

3.3. PSY shifts phase equilibrium in lipid bilayers

We further explored whether the PSY-induced phase equilibrium perturbation observed in heterogeneous Langmuir films was also present in bilayer membranes. For this purpose, we formed giant uni-lamellar liposomes (GUVs) of pure phospholipids or composed by the MM mixture.

GUVs composed of pure DMPC were chosen as model membranes because they show a gel to liquid-crystalline (or liquid-disordered; LD) phase transition at room temperature (melting temperature,
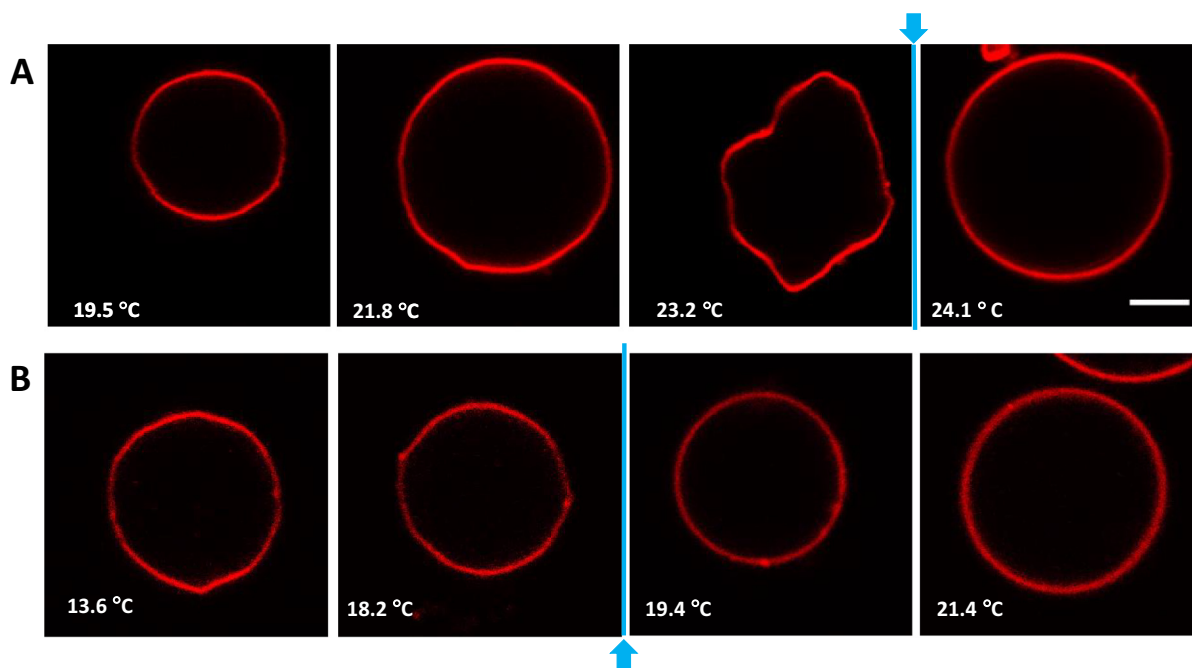
Fig. 5. Confocal microscopy images of GUVs. Representative vesicles observed in the equatorial plane, composed of DMPC (A) and DMPC in the presence of 25 mol% of PSY (B) are shown at the indicated temperature. For both lipid systems, 0.5 mol% of PE-Rho was added for membrane visualization. The images are representative of > 50 vesicles analyzed. The arrows indicate the temperature interval in which the vesicles adopt a circular shape. Scale bar is 5 µm.

Tm = 23.9 °C, [30]). Confocal microscopy of DMPC GUVs showed a change in the vesicle shape during the slow heating of the sample (~10 °C/h) near its Tm (Fig. 5). This effect has been previously reported in an early observation of GUVs composed of DMPC and other PC of longer acyl chains [31]. We found that the vesicles show non-circular shapes and little shape fluctuation when maintained below their Tm, evidencing the presence of a rigid lipid phase. When approaching the vicinity of the phase transition temperature (within 0.5 °C), we observed an increase in the vesicles' shape fluctuation (see image time series in figure S3_A and S3_B, in Supplementary material - *II*)) and an absence of defined angles in the circumference. Above 24.0 ± 0.2 °C, the vesicles appeared circular and showed low shape fluctuation.

When GUVs of DMPC were formed in the presence of 25 mol% of PSY, a similar effect was observed but shifted to lower temperatures (Fig. 5). Non-circular shapes were observed below 19.0 ± 0.5 °C, and circular shapes above this temperature. This indicates that PSY induces a lowering of the vesicle Tm by ~5 °C, likely by partition preferentially into the LD phase and increasing its thermodynamic stability. This effect agrees with the observation of an increase in the surface pressure range of the isothermal phase transition of DPPC monolayers (Fig. 3) and supports a preferential partition of PSY into the more fluid phase.

We also explored the effect of PSY on the lateral phase organization of giant vesicles composed by the MM mixture. Confocal microscopy shows, in most of the vesicles analyzed, images that strongly resemble liquid-liquid coexistence (Figs. 6 and S4 in Supplementary material - *II*). This pattern matches that previously observed in vesicles containing sphingolipids and CHO [32,33]: the fluorescent probe concentrates in the LD phase and is poorly present in the LO phase, showing a difference in fluorescence intensity between the phases.

Yurlova et al. have shown that myelin lipids from wild-type mice laterally segregate into physically distinct lipid phases in GUVs, but form homogeneous membranes when they are composed of lipids from mice that do not synthesize compact myelin [34]. Our findings using a lipid mixture mimicking myelin closely reproduced those observations.

The addition of 25 mol% of PSY to the MM lipids results in vesicles with a higher proportion of homogeneous vesicles (Figs. 6 and S4), which is typically found in LD membranes such as those composed of

phospholipids containing < 15 mol% of CHO [32]. Then, in agreement with the observation in monolayers composed of the MM mixture (Fig. 4), PSY also had the capacity in bilayer membranes to shift the phase equilibrium of the complex mixture that mimics myelin. Here, its effect resulted in the promotion of the occurrence of homogeneous vesicles, disrupting lipid domains.

3.4. Effect of PSY on surface electrostatics

Due to the importance of the electrostatic properties of membranes in the structure and organization of myelin, we further explored the effect of PSY on the surface structuring and electrostatics. Surface potential difference relative to water is a complex property. This represents the electrical potential profile across the interface between the bulk aqueous phase and the hydrocarbon region that arises from the dipole moment of the lipid components, also having contributions from the surface-associated water [21,35]. All natural lipids have a dipole moment perpendicular to the interface, with its positive extreme to the nonpolar portion of the lipids (hydrocarbon chains) and a negative pole to the water phase [35] (see Scheme 2). When the lipid monolayers have a formal charge, this also contributes to the total amount measured as surface potential, as well as their associated counter-ions and electrical double layer [21,35].

Our measurement of surface potential for pure PSY gave values of 360 ± 5 mV, which agrees with previous reports [10]. Then, even for a cationic monolayer composed of a partially charged lipid, the resultant perpendicular dipole still has its positive pole towards the acyl chains due to a more important contribution of the acyl chains to the total value, as has been previously reported [35]. Neutral phospholipid monolayers [35,36], as well as the negatively charged MM membrane, showed higher surface potential, evidencing a larger molecular dipole (Fig. 7A) than PSY alone.

In this work, we were concerned with the effect of surface charge introduced by 25 mol% of PSY on the surface electrostatics. We observed that, in high salt conditions, all membranes exhibited a modest increase of surface potential in the presence of PSY (not shown). With the purpose of exacerbating the charge double-layer effect over the
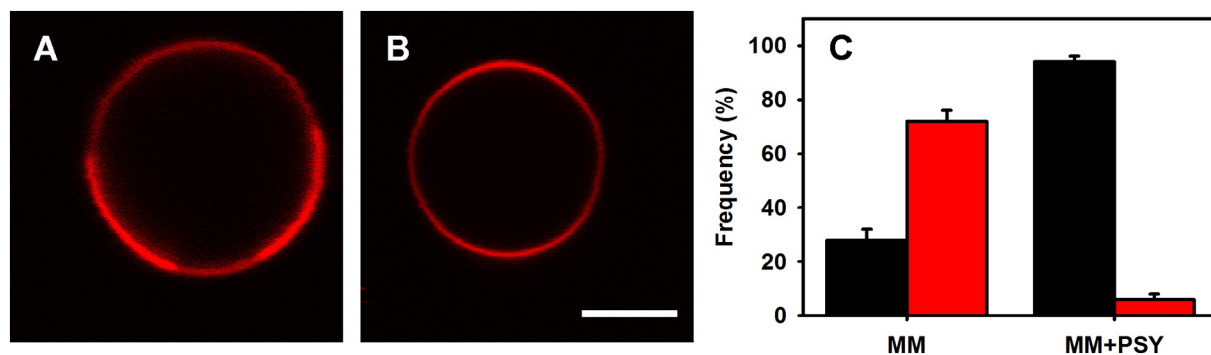
Fig. 6. Confocal microscopy images of GUVs. The images show representative vesicles in the equatorial plane, composed of MM showing segregated domains (A) or a homogenous pattern (B). For both lipid systems, 0.5 mol% of PE-Rho was added for membrane visualization. C) Percent frequency of the occurrence of homogeneous vesicles (black bars) or containing lipid domains (red bars) in the GUVs composed of the myelin mimic mixture without (MM) and with (MM + PSY) the addition of 25 mol% PSY. The data corresponds to the average of the absolute frequency of a structural type normalized by sample size (40–45 vesicles/condition) and the error bars correspond to the SEM. Scale bar is 5 μm.

molecular dipole due to the hydrocarbon portion [35], we worked in low ionic conditions. In this environment, the lipid films showed enhanced surface potential, and introducing 25 mol% of PSY resulted in even higher values, most evident in the anionic MM films (Fig. 7A). This indicates that PSY did not reduce the surface potential, making the water side of the membrane more positive as expected, but the contrary. We therefore studied the different actors contributing to the surface electrostatics by different approaches.

Zeta potential is the electric potential at the shear plane of a particle, which is the plane defining what migrates in the electric field [37]. Thus, zeta potential measures long-range electrostatic potential

and is not influenced by local dipole effects at the interface. Phospholipid liposomes are known to show negative zeta potentials due to selective surface adsorption of ions, which depends on temperature and ionic conditions as well as the buffer molecule used [37–40]. Our results showed negative values of zeta potential for large unilamellar vesicles (LUVs) composed of POPC and DPPC, as reported previously [40], and more negative values for the anionic MM membranes, as expected for its anionic nature (Fig. 7B). The sign and magnitude of zeta potential of DPPC liposomes has been reported to be determined by a net ion accumulation on the liposome surface [40] and a reorientation of the head group due to phase state and ionic conditions [38].
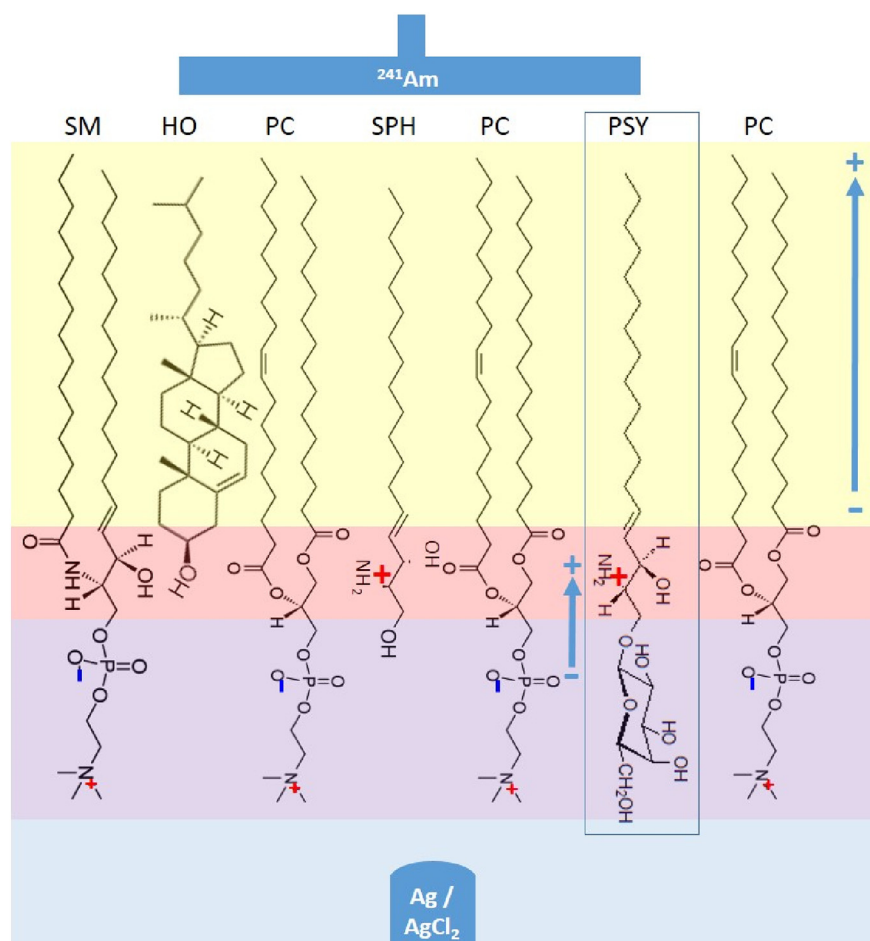
Scheme 2. Schematic representation of a hypothetical distribution of PSY, SPH, sphingomyelin (SM) and CHO immersed in a PC membrane: the positioning of the cationic lipids in the glycerol group layer may explain the increase in surface potential of PSY-containing membranes. The colored boxes represent the hydrophobic membrane section (yellow), the interfacial section that contains the glycerol group (pink), the polar group section (purple) and the bulk water (light blue). The Ag/AgCl₂ and [241]Am electrodes used for surface potential measurements are represented in blue. The arrows represent the direction of the dipoles that contribute to the surface potential measurements of monolayers.
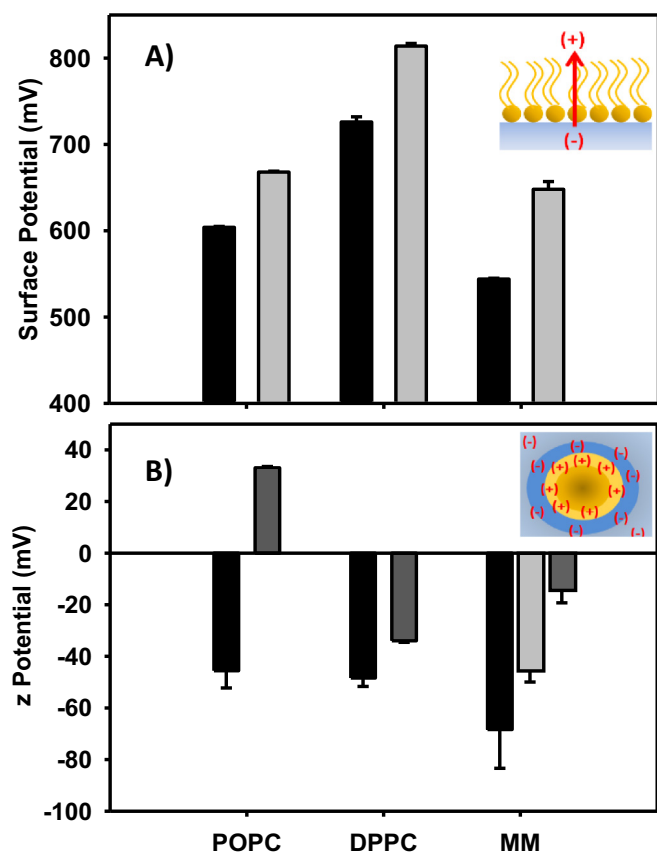
Fig. 7. Electrostatic effect of PSY on lipid membranes. A) Surface potential of lipid monolayers at 30 mN/m in the absence (black bars) or presence (gray bars) of 25 mol% of PSY. B) zeta potential of extruded lipid suspension (0.4 mM) in the absence (black bars) or presence of 10 (light gray bar, only for MM membranes) or 25 mol% (dark gray bars) of PSY. The experiments were performed in low salt conditions and pH 7.4, T: 22 ± 1 °C. Lipid composition was POPC, DPPC or myelin-like mixture (MM), as indicated. The data are the average of three independent experiments. Error bars represent SEM.

The addition of PSY to any of the liposome preparations resulted in a shift to more positive zeta potential values. For phospholipid vesicles, PSY showed a more important effect on POPC than on DPPC LUVs. This may be the consequence of a lower incorporation of PSY on DPPC membranes. DPPC monolayers showed saturation at lower PSY mole fraction (X_{50}) than POPC (Fig. 2), and PSY was nearly excluded from DPPC films in the LC state (Fig. 3, S1). Here, LUVs formed by DPPC were below its Tm and were present in the gel state [25], which is equivalent to the LC phase described in monolayers.

Additionally, DPPC-PSY buffer suspensions were the only samples showing micelle-size particles by DLS (data not shown), probably enriched in PSY, suggesting the exclusion of PSY from the lipid membrane. MM LUVs were highly affected by the presence of PSY. In this case, the anionic lipid membrane may accept enough of the cationic PSY to nearly neutralize the zeta potential, probably being stabilized at the membrane surface by forming salt bridges.

To further understand how PSY interacts with these lipid bilayers, we measured Laurdan GP and fluorescence anisotropy of DPH, which provide complementary information about membrane surface hydration and membrane fluidity. The surface water structuring was studied through the fluorescent behavior of Laurdan, a dye sensitive to the hydration of the lipid interface [41]. Laurdan spontaneously partitions into the interfacial region where the phospholipid headgroup locates, and its fluorescence is strongly influenced by the dipolar relaxation of the water molecules and the dynamic of rotation of dipoles in this region, reflecting the local viscosity. The generalized polarization

function of Laurdan (GP; Eq. (5)) makes it possible to infer whether the presence of PSY can alter the interfacial properties of the lipid vesicles. We used multilamellar lipid vesicles (MLVs) for Laurdan experiments, because their regular lamellar organization closely resembles the natural organization of myelin [13]. Additionally, the interlamellar structure of myelin is known to be regulated by the electrostatic properties of the surfaces interacting and the thin layer of structured water between them [13,42].

DPPC gives high values of GP, as expected for a phospholipid membrane in the gel state. Phospholipids in the LD phase, such as POPC, are expected to show low GP values, due to the relaxation of the surface water that matches the loosening of van der Waals interactions of the acyl chains [41]. For myelin lipid membranes, high GP values were reported [34], evidencing highly ordered surface water and local viscosity. Our results (Table S1, in Supplementary material - I) agree with the literature for all three lipid systems used [34,41,43].

Laurdan fluorescence measurements of PSY buffer suspension give rather low GP values (close to zero), which match the expanded character observed in monolayer systems. However, when 25 mol% of PSY is present in the lipid MLVs suspensions, this does not decrease GP, but causes no effect or even increases it (Table S1). For DPPC, no significant change is evident, again probably because of low integration of PSY into the lipid bilayer in the gel phase. On the other hand, POPC membranes containing PSY clearly behave as more structured or viscous at the interface, from the presence of a charged surface. This agrees with previous reports of an increase of Laurdan GP induced by PSY in red blood cells or oligodendrocyte culture [1]. For MM membranes, the small increase observed in GP may be a consequence of the structuring of water and/or higher local viscosity induced by high local electrostatic fields resulting from the presence of both anionic and cationic components at the membrane surface. This indicates that PSY has an ordering effect on the polar surface of the membrane that does not match the loosening of the ordering of acyl chains evidenced by the decrease of Cs^{-1} in monolayers (see Fig. S2B).

The steady anisotropy of DPH in MLVs was measured to assess the effect of PSY on the mobility of membrane lipids. DPH is a fluorophore that locates in the hydrophobic core of the bilayer, is oriented predominantly parallel to the fatty acid chains of the phospholipids [17,43], and is sensitive to changes in the microviscosity of the hydrophobic portion of the lipid membrane. An increase in the amount of unsaturated fatty acid of phospholipids is expected to decrease the anisotropy of DPH [17], and we did observe a lower fluorescence anisotropy value for POPC MLVs compared to DPPC [43] or MM membranes (Table S1). An addition of 25 mol% of PSY did not induce any appreciable change, which matches the recently reported lack of change in the fluorescence anisotropy of the related probe TMA-DPH after the addition of PSY to cell membranes [1]. An increase of DPH anisotropy has been reported after adding 10 mol% of the chemically related sphingolipid SPH to model lipid membranes [44], which has been interpreted as the bilayer becoming more rigid as a result of sphingosine incorporation. The authors stated that, even though the increase in DPH anisotropy was small (typically of 0.01–0.02 polarization units), it was highly reproducible. Our results also show this small increase for all three lipid membranes studied (Table S1). Unfortunately, our experimental configuration lacks the necessary sensitivity to ensure a statistically significant difference in these measurements. This parameter appears to reflect the moderate surface structuring induced by PSY but not the increase in elasticity observed for Langmuir monolayers. The latter parameter evidences the macroscopic (average) rheological character of the membrane, as it is a direct measurement of the entropy of compression (not of the fluidity of the film). On the other hand, fluorescence anisotropy measurements reflect the molecular environment of the probe, being sensitive to the local microviscosity. Even for most lipid membranes, both parameters are often found in parallel, describing different aspects of the film and at different scale levels. The overall picture suggests that the membrane

system has an interesting dislocation between macroscopic elasticity and local microviscosity. This may arise from an anchorage of the cationic head group of PSY between the anionic lipids or the local charges of phospholipid, which restricts lateral mobility but not the conformational freedom of the hydrocarbon tail.

4. General discussion

At neutral pH, which corresponds to the environmental conditions for PSY in a pathological situation, PSY is surface active, being able to lower the surface tension of water from ~72 to ~32 mN/m and showing a CMC of 38 ± 3 μM. This value is ~30 times lower than the reported CMC at pH 4 [9], evidencing a more hydrophobic character at neutral pH. In the latter conditions, PSY organizes in large structures, probably lamellar in nature, in equilibrium with a small proportion of micelles. From the mean molecular area obtained by surface activity experiments and applying the concepts and equations proposed by Israelachvilli about amphiphile geometry [45], we calculated a critical packing parameter of 0.6 for PSY, which is close to the reported value for the closely related cationic lipid SPH (0.49; [46]). This value falls in the critical packing parameter range (0.5–1.0) that corresponds to amphiphiles forming planar arrangements such as multilamellar structures. PSY films are easily compressed, evidencing a loose packing of their acyl chains. However, the surface of those structures, which interacts with water where a net positive charge is present, shows certain structuring evidenced by a relatively high Laurdan GP value. The overall picture agrees with the fact that PSY accumulates in the extracellular milieu of brain in Krabbe's disease, probably structured in a similar way.

When integrated into phospholipid membranes, PSY shows a high sensitivity to the phase state. It partitions preferentially to the more disordered phases of both monolayer and bilayer systems, affecting phase equilibrium in a similar way to that described for other mild soluble amphiphiles and amphipathic peptides [47]. However, when PSY was incorporated into condensed phospholipid phases, it affected its rheological as well as its topological organization. It is notable that SPH induces the opposite effect on DPPC bilayers, stabilizing the gel phase and increasing the Tm [48]. This may be a consequence of the smaller polar group of SPH, which may favor closer packing of the acyl chains.

A high PSY concentration was used in the present work to highlight its effect on the physical properties of the membrane. A 100-fold higher concentration of PSY (~90 pmol/mg prot) was found in myelin of a murine model for Krabbe's disease than in normal myelin [1]. Bearing in mind that myelin proteins account for only 25% of the myelin dry weight, the rest being mainly lipids [13], this indicates an enrichment of up to 1.5 mol% of PSY among myelin lipids in pathological conditions. However, further local concentration of PSY may occur if lipid distribution is not homogeneous among the cell membranes or concentrates in particular tissue locations. Our results highlight a favored incorporation of PSY into the more fluid phases of phospholipid membranes when present at 25 mol%, evidenced by the alteration of the phospholipid phase behavior. Nevertheless, this preference should also occur even if PSY is present at much lower concentrations.

For membranes composed of myelin lipids (MM), PSY also shows preference for one of the coexistent phases. Monolayer experiments suggest that PSY prefers the expanded phase, increasing the composition miscibility gap and stabilizing phase separation in Langmuir films. PSY also induces lipid domain disruption in lipid bilayers inducing the occurrence of homogeneous vesicles, as observed by confocal microscopy. The phase character of such vesicles was not studied, since no CHO effect experiments were performed. Nevertheless, this finding evidences a clear preferential partition of PSY and the thermodynamic stabilization of one lipid phase to the detriment of the other [47]. Thus, PSY potentiality affects the subtle balance that regulates phase separation in myelin [34,42]. Even though our lipid model systems are far

from the complexity of cell membranes, our results match recent reports of PSY as capable of decreasing the occurrence of sub-micrometric domains in red blood and oligodendrocyte cells [1], providing thermodynamic support for such a process.

The accumulation of PSY in the brain in the murine model of Krabbe's disease has been reported to be related to lipid rafts [6]. These are entities proposed to exist in biomembranes and would show the LO phase due to their high content of CHO. PSY was co-isolated with CHO in membrane fractions and raft protein markers were altered. Our results with MM membranes suggest that phase separation may be altered by PSY in myelin membranes. Myelin phase separation is known to be subtly regulated by the presence of salts, both in Langmuir films as well as in multilamellar bilayer structures [34,42]. The addition of a cationic molecule such as PSY to myelin may alter the surface electrostatic balance, which may contribute to the driving force for phase separation and redistribution of components, as has been observed in the presence of ions [42] or evidenced by raft studies [6].

Pioneer works report that the demyelinating disease, multiple sclerosis, lowered (by 13 °C) the phase transition temperature of liposomes composed of myelin lipids [49]. Also, myelin vesicles of murine mutants that are unable to form stable myelin showed a less ordered membrane than the wild-type and a lack of lipid domains [34]. Demyelination in these diseases involves the breakdown of large quantities of phospholipids [49]. Considering that the activity of several phospholipases, and in particular of sphingomyelinase, strongly depends on the presence of an LD phase [50,51], stabilization of the LD phase against the LO phase by the presence of PSY may induce an increase in phospholipase activity, threatening myelin membrane stability.

The surface electrostatics of lipid membranes is altered by PSY in a complex manner. PSY adds a positive net charge to the membrane surface, evidenced by more positive values of zeta potential, but structures the surface water. This effect results in an enhanced dipole perpendicular to the membrane, with its positive end to the acyl chains, as evidenced by surface potential measurements. It can be explained by considering the probable molecular organization of the polar portion of the cationic PSY among zwitterionic PC molecules at the head group level. Scheme 2 represents a hypothetical distribution of PSY along the different layers of a lipid film of several molecules studied in the present work or chemically related. The cationic molecules PSY and SPH can be accommodated placing the positive charge in the interfacial section along the glycerol groups of PC and the amide group of sphingolipids. Thus, a positively charged layer is established above the phosphate layer and opposite to the positively charged choline groups. The contribution of the cationic lipids results in a larger overall dipole perpendicular to the membrane plane, increasing the surface potential values (Scheme 2 and Fig. 7). On the other hand, the addition of this third ionic layer to the interfacial section will add surface structuring revealed as greater Laurdan GP values.

Early theoretical calculations demonstrated that zwitterionic molecules such as DPPC can reorient their polar heads as a response to changes in ionic strength [38]. At a low ionic strength, the choline groups are located below the phosphate group, whilst an outward exposure of phosphate groups is evidenced in high salt conditions. Therefore, some flexibility in the orientation of the choline headgroup should be expected because of the addition of cationic lipids, an effect that would further influence the membrane surface electrostatics.

In summary, the effect of PSY on surface electrostatics induces a dual effect on overall lipid membrane behavior: it reduces the compactness of the hydrophobic portion, making the membrane more easily compressed, and concomitantly enhances surface structuring by introducing a net positive charge, which may establish structured ionic layers at the interfacial region of phospholipid membranes as well as salt bridges with the anionic lipid components of myelin.

Transparency document

The Transparency document associated with this article can be found, in online version.

Acknowledgments

This work was supported by the Consejo Nacional de Investigaciones Científicas y Técnicas (CONICET), Agencia Nacional de Promoción Científica y Tecnológica (ANPCyT, FONCyT PICT 2014-1627), and the Secretary of Science and Technology of Universidad Nacional de Córdoba (SECyT-UNC) Argentina to M.L.F. and NIH R01 NS065808 to E.R.B. Y.M.Z.D. is a CONICET fellow; M.L.F. is Career Researcher of CONICET-UNC. The microscopy experiments were performed at the Centro de Micro y Nanoscopía de Córdoba (CEMINCO), working as part of the "Sistema Nacional de Microscopía (SNM-MINCyT)". The authors thank Dr. Maria Soledad Celej and Dr. Ernesto Ambroggio for useful discussions and Dr. Bruno Maggio for the generous gift of purified myelin sphingolipids.

Author contributions

The experimental work was performed by Y.M.Z.D and S.C. The project was designed by M.L.F and E.B and directed by M.L.F. The manuscript was written through contributions of all authors. All authors have given approval to the final version of the manuscript.

Appendix A. Supplementary data

Supplementary data to this article can be found online at https://doi.org/10.1016/j.bbamem.2018.09.015.

References

[1] L. D'Auria, C. Reiter, E. Ward, A.L. Moyano, M.S. Marshall, D. Nguyen, et al., Psychosine enhances the shedding of membrane microvesicles: implications in demyelination in Krabbe's disease, PLoS One 12 (2017) 1–19, https://doi.org/10.1371/journal.pone.0178103.

[2] E.R. Bongarzone, M.L. Escolar, S.J. Gray, T. Kafri, C.H. Vite, M.S. Sands, Insights into the pathogenesis and treatment of Krabbe disease, Pediatr. Endocrinol. Rev. 13 (Suppl. 1) (2016) 689–696 http://www.ncbi.nlm.nih.gov/pubmed/27491217.

[3] J. A Hawkins-Salsbury, A.R. Parameswar, X. Jiang, P.H. Schlesinger, E. Bongarzone, D.S. Ory, et al., Psychosine, the cytotoxic sphingolipid that accumulates in globoid cell leukodystrophy, alters membrane architecture, J. Lipid Res. 54 (2013) 3303–3311, https://doi.org/10.1194/jlr.M039610.

[4] Y. A Hannun, R.M. Bell, Functions of sphingolipids and sphingolipid breakdown products in cellular regulation, Science 243 (1989) 500–507, https://doi.org/10.1126/science.2643164.

[5] L. D'Auria, E.R. Bongarzone, Fluid levity of the cell: role of membrane lipid architecture in genetic sphingolipidoses, J. Neurosci. Res. 94 (2016) 1019–1024, https://doi.org/10.1002/jnr.23750.

[6] A.B. White, M.I. Givogri, A. Lopez-Rosas, H. Cao, R. van Breemen, G. Thinakaran, et al., Psychosine accumulates in membrane microdomains in the brain of krabbe patients, disrupting the raft architecture, J. Neurosci. 29 (2009) 6068–6077, https://doi.org/10.1523/JNEUROSCI.5597-08.2009.

[7] T. Heimburg, Thermal Biophysics of Membranes, WILEY-VCH Verlag GmbH & Co. KGaA, Germany, 2007.

[8] F.M. Goñi, A. Alonso, Biophysics of sphingolipids I. Membrane properties of sphingosine, ceramides and other simple sphingolipids, Biochim. Biophys. Acta Biomembr. 1758 (2006) 1902–1921, https://doi.org/10.1016/j.bbamem.2006.09.011.

[9] L. Orfi, C.K. Larive, S.M. LeVine, Physicochemical characterization of psychosine by _1_H nuclear magnetic resonance and electron microscopy, Lipids 32 (1997) 1035–1040.

[10] B. Maggio, F.A. Cumar, R. Caputto, Surface behaviour of gangliosides and related glycosphingolipids, Biochem. J. 171 (1978) 559–565.

[11] R.G. Oliveira, R.O. Calderon, B. Maggio, Surface behavior of myelin monolayers, BBA. 1370 (1998) 127–137.

[12] C.M. Rosetti, B. Maggio, R.G. Oliveira, The self-organization of lipids and proteins of myelin at the membrane interface. Molecular factors underlying the microheterogeneity of domain segregation, Biochim. Biophys. Acta Biomembr. 1778 (2008) 1665–1675, https://doi.org/10.1016/j.bbamem.2008.02.007.

[13] C.S. Raine, Morphology of myelin and myelination, in: P. Morell (Ed.), Myelin, Second Ed, Springer Science + Business Media, LLC, New York, 1984, pp. 1–50.

[14] Y. de las M. Zulueta Díaz, M. Mottola, R.V. Vico, N. Wilke, M.L. Fanani, The

[15] R. Maget-Dana, The Monolayer Technique: A Potent Tool for Studying the Interfacial Properties of Antimicrobial and Membrane-lytic Peptides and Their Interactions With Lipid Membranes, (1999), https://doi.org/10.1016/S0005-2736(99)00203-5.

[16] D. Vollhardt, Brewster angle microscopy: a preferential method for mesoscopic characterization of monolayers at the air/water interface, Curr. Opin. Colloid Interface Sci. 19 (2014) 183–197, https://doi.org/10.1016/j.cocis.2014.02.001.

[17] J.R. Lakowicz, Fluorescence anisotropy, Princ. Fluoresc. Spectrosc. Third Ed., Plenum Publishers, New York, 2006, pp. 353–381.

[18] J.A. Bellon, M. Pino, N. Wilke, Low-cost equipment for electroformation of Giant Unilamellar Vesicles, HardwareX 4 (2018) e00037, , https://doi.org/10.1016/j.ohx.2018.e00037.

[19] W.R. Hargreaves, D.W. Deamer, Liposomes from ionic, single-chain amphiphiles, Biochemistry 17 (1978) 3759–3768, https://doi.org/10.1021/bi00611a014.

[20] R. Koynova, M. Caffrey, Phases and phase transitions of the sphingolipids, Biochim. Biophys. Acta Rev. Biomembr. 1255 (1995) 213–236, https://doi.org/10.1016/S0304-4157(98)00006-9.

[21] R.E. Brown, H.L. Brockman, Using monomolecular films to characterize lipid lateral interactions, Methods Mol. Biol. 398 (2007) 41–58, https://doi.org/10.1007/978-1-59745-513-8_5.

[22] S. Ali, J.M. Smaby, M.M. Momsen, H.L. Brockman, R.E. Brown, Acyl chain-length asymmetry alters the interfacial elastic interactions of phosphatidylcholines, Biophys. J. 74 (1998) 338–348, https://doi.org/10.1016/S0006-3495(98)77791-4.

[23] J.T. Davies, E.K. Rideal, Interfacial Fenomena, (1963).

[24] M.L. Fanani, B. Maggio, Liquid−liquid domain miscibility driven by composition and domain thickness mismatch in ternary lipid mixtures, J. Phys. Chem. B 115 (2011) 41–49, https://doi.org/10.1021/jp107344t.

[25] Y. de las M. Zulueta Díaz, M.L. Fanani, Crossregulation between the insertion of Hexadecylphosphocholine (miltefosine) into lipid membranes and their rheology and lateral structure, Biochim. Biophys. Acta Biomembr. 1859 (2017) 1891–1899, https://doi.org/10.1016/j.bbamem.2017.06.008.

[26] R.M. Weis, H.M. McConnel, Two-dimensional chiral crystals of phospholipid, Nature 310 (1984) 47–49.

[27] P. Krüger, M. Lösche, Molecular chirality and domain shapes in lipid monolayers on aqueous surfaces, Phys. Rev. E Stat. Phys. Plasmas Fluids Relat. Interdiscip. Topics 62 (2000) 7031–7043, https://doi.org/10.1103/PhysRevE.62.7031.

[28] H.M. McConnell, Harmonic shape transitions in lipid monolayer domains, J. Phys. Chem. 794 (1990) 4728–4731.

[29] R.G. Oliveira, B. Maggio, Compositional domain immiscibility in whole myelin monolayers at the air-water interface and Langmuir-Blodgett films, Biochim. Biophys. Acta Biomembr. 1561 (2002) 238–250, https://doi.org/10.1016/S0005-2736(02)00350-4.

[30] T.B. Pedersen, S. Frokjaer, O.G. Mouritsen, K. Jørgensen, A calorimetric study of phosphocholine membranes mixed with desmopressin and its diacylated prodrug derivative (DPP), Int. J. Pharm. 233 (2002) 199–206, https://doi.org/10.1016/S0378-5173(01)00946-2.

[31] L.A. Bagatolli, E. Gratton, Two-photon fluorescence microscopy observation of shape changes at the phase transition in phospholipid giant unilamellar vesicles, Biophys. J. 77 (1999) 2090–2101, https://doi.org/10.1016/S0006-3495(99)77050-5.

[32] S.L. Veatch, S.L. Keller, Seeing spots: complex phase behavior in simple membranes, Biochim. Biophys. Acta, Mol. Cell Res. 1746 (2005) 172–185, https://doi.org/10.1016/j.bbamcr.2005.06.010.

[33] D.D.S. Alvares, J. Ruggiero Neto, E.E. Ambroggio, Phosphatidylserine lipids and membrane order precisely regulate the activity of Polybia-MP1 peptide, Biochim. Biophys. Acta Biomembr. 1859 (2017) 1067–1074, https://doi.org/10.1016/j.bbamem.2017.03.002.

[34] L. Yurlova, N. Kahya, S. Aggarwal, H.J. Kaiser, S. Chiantia, M. Bakhti, et al., Self-segregation of myelin membrane lipids in model membranes, Biophys. J. 101 (2011) 2713–2720, https://doi.org/10.1016/j.bpj.2011.10.026.

[35] V. Vogel, D. Möbius, Local surface potentials and electric dipole moments of lipid monolayers: contributions of the water/lipid and the lipid/air interfaces, J. Colloid Interface Sci. 126 (1988) 408–420, https://doi.org/10.1016/0021-9797(88)90140-3.

[36] C.B. Casper, D. Verreault, E.M. Adams, W. Hua, H.C. Allen, Surface potential of DPPC monolayers on concentrated aqueous salt solutions, J. Phys. Chem. B 120 (2016) 2043–2052, https://doi.org/10.1021/acs.jpcb.5b10483.

[37] M. Eisenberg, T. Gresalfi, S. McLaughlin, Adsorption of monovalent cations to bilayer membranes containing negative phospholipids, Biochemistry 18 (1979) 5213–5223.

[38] K. Makino, T. Yamada, M. Kimura, T. Oka, H. Ohshima, T. Kondo, Temperature-and ionic strength-induced conformational changes in the lipid head group region of liposomes as suggested by zeta potential data, Biophys. Chem. 41 (1991) 175–183, https://doi.org/10.1016/0301-4622(91)80017-L.

[39] D.J.A. Crommelin, Influence of lipid composition and ionic strength on the physical stability of liposomes, J. Pharm. Sci. 73 (1984) 1559–1563.

[40] E. Chibowski, A. Szcześ, Zeta potential and surface charge of DPPC and DOPC liposomes in the presence of PLC enzyme, Adsorption 22 (2016) 755–765, https://doi.org/10.1007/s10450-016-9767-z.

[41] T. Parasassi, G. De Stasio, A. D'Ubaldo, E. Gratton, Phase fluctuation in phospholipid membranes revealed by Laurdan fluorescence, Biophys. J. 57 (1990) 1179–1186, https://doi.org/10.1016/S0006-3495(90)82637-0.

[42] R.G. Oliveira, E. Schneck, S.S. Funari, M. Tanaka, B. Maggio, Equivalent aqueous

phase modulation of domain segregation in myelin monolayers and bilayer vesicles, Biophys. J. 99 (2010) 1500–1509, https://doi.org/10.1016/j.bpj.2010.06.053.

[43] S.N. Pinto, F. Fernandes, A. Fedorov, A.H. Futerman, L.C. Silva, M. Prieto, A combined fluorescence spectroscopy, confocal and 2-photon microscopy approach to re-evaluate the properties of sphingolipid domains, Biochim. Biophys. Acta Biomembr. 1828 (2013) 2099–2110, https://doi.org/10.1016/j.bbamem.2013.05.011.

[44] F.X. Contreras, J. Sot, A. Alonso, F.M. Goñi, Sphingosine increases the permeability of model and cell membranes, Biophys. J. 90 (2006) 4085–4092, https://doi.org/10.1529/biophysj.105.076471.

[45] J.N. Israelachvili, Soft and biological structures, Intermol. Surf. Forces, 2011, pp. 535–576, , https://doi.org/10.1016/B978-0-12-375182-9.10020-X.

[46] M.A. Perillo, A. Polo, A. Guidotti, E. Costa, B. Maggio, Molecular parameters of semisynthetic derivatives of gangliosides and sphingosine in monolayers at the air-water interface, Chem. Phys. Lipids 65 (1993) 225–238, https://doi.org/10.1016/0009-3084(93)90020-4.

[47] M.L. Fanani, N. Wilke, Regulation of phase boundaries and phase-segregated patterns in model membranes, Biochim. Biophys. Acta Biomembr. (2018), https://doi.org/10.1016/j.bbamem.2018.02.023.

[48] A. Kõiv, P. Mustonen, P.K.J. Kinnunen, Influence of sphingosine on the thermal phase behaviour of neutral and acidic phospholipid liposomes, Chem. Phys. Lipids 66 (1993) 123–134, https://doi.org/10.1016/0009-3084(93)90037-4.

[49] L.S. Chia, J.E. Thompson, M.A. Moscarello, Alteration of lipid-phase behavior in multiple sclerosis myelin revealed by wide-angle X-ray diffraction, Proc. Natl. Acad. Sci. 81 (1984) 1871–1874, https://doi.org/10.1073/pnas.81.6.1871.

[50] F.X. Contreras, J. Sot, M.B. Ruiz-Argüello, a. Alonso, F.M. Goñi, Cholesterol modulation of sphingomyelinase activity at physiological temperatures, Chem. Phys. Lipids 130 (2004) 127–134, https://doi.org/10.1016/j.chemphyslip.2004.02.003.

[51] L. De Tullio, B. Maggio, M.L. Fanani, Sphingomyelinase acts by an area-activated mechanism on the liquid-expanded phase of sphingomyelin monolayers, J. Lipid Res. 49 (2008) 2347–2355, https://doi.org/10.1194/jlr.M800127-JLR200.